

Third European Rotorcraft and Powered-Lift Aircraft Forum

Paper No. 22

**Helicopter Vibration Reduction With
Higher Harmonic Blade Pitch**

Frank J. McHugh and John Shaw

Boeing Vertol Company
Philadelphia, Pennsylvania, USA

September 7-9, 1977

Aix-en-Provence, France

Association Aeronautique et Astronautique de France



HELICOPTER VIBRATION REDUCTION
WITH HIGHER HARMONIC BLADE PITCH

Frank J. McHugh and John Shaw
Boeing Vertol Company

Abstract

A wind-tunnel test supported by theoretical analysis has been used to evaluate higher harmonic blade pitch for the reduction of helicopter vibration. This investigation focuses on the hingeless rotor and is a continuation of work reported previously. The new results are the first obtained for higher harmonic pitch on a hingeless rotor at close to full-scale tip speed, with blade dynamic characteristics properly modeled. This was also the first successful exploration of vibratory hub-moment reduction using higher harmonic pitch on a fully instrumented model.

Results of this testing were very favorable. The higher harmonic pitch was found to be easily adjustable for the desired reductions in vibratory hub loads. All hub-load components--forces and moments--could be reduced simultaneously using higher harmonic inputs to the swashplate. There were no significant penalties in blade flap-bending loads or performance. Pitch amplitudes necessary to eliminate vibratory hub moments were in the practical range, although beyond the current capability of the model. Testing at various flight conditions showed that higher harmonic amplitude and phase requirements change significantly with speed. It appears, as expected, that in-flight adjustment of these parameters will be required.

Notation

Harmonic waveforms are described in this paper according to the following convention. An n /rev variation of a parameter x is written as

$$x_n(\psi) = |x_n| \cos(n\psi - \phi_n),$$

in which $|x_n|$ = harmonic amplitude

ϕ_n = harmonic phase

ψ = blade azimuth

n = harmonic number

The abbreviated notation A/ϕ is used in referring to a harmonic waveform of amplitude A and phase ϕ .

Other notation follows.

b number of blades

C_T rotor thrust coefficient, $T/\rho(\Omega R)^2 \pi R^2$

c	blade chord, m (ft)
d	rotor diameter, m (ft)
M_β	flap-bending moment, n-m (in.-lb)
q	dynamic pressure, $\rho V^2/2, n/m^2$ (lb/ft ²)
R	rotor radius, m (ft)
r	blade element radius, m (ft)
V	flight speed, m/sec (ft/sec)
X	rotor propulsive force, n (lb)
α_s	rotor shaft angle, degrees
θ	blade pitch angle, degrees
μ	rotor advance ratio, $V \cos \alpha_s / \Omega R$
ρ	air density, kg/m ³ (slug/ft ³)
σ	rotor solidity, $bc/\pi R$
Ω	rotor shaft speed, rad/sec

Subscripts

c	cosine component
s	sine component

1. Introduction

Higher harmonic blade pitch has long been an attractive but undeveloped approach to the reduction of vibratory rotor loads and the resultant airframe vibration. The concept is straightforward. Most helicopter vibration originates in the nonuniform velocity distribution encountered by the rotor blades as they travel around the azimuth. This nonuniform distribution is due to the constantly changing orientation of the blades relative to the direction of flight and the irregular vortex wake beneath the rotor. The resulting variation of blade angle of attack with azimuth contains every harmonic of rotor shaft speed. Only certain harmonics, however, cause vibratory loads which are transmitted to the fuselage. Many harmonics produce loads on the various blades which cancel each other completely in combining at the hub. Higher harmonic blade pitch, superimposed on the conventional zero and one-per-rev blade pitch control, is a means of selectively controlling the harmonics of angle of attack which do produce vibration.

Wind-tunnel tests, a short flight test, and theoretical studies¹⁻⁹ have been conducted to evaluate this concept. The overall conclusion has been

Copies of this paper are available from the Technical Library, Boeing Vertol Company, Box 16858, Philadelphia, Pennsylvania, 19142, USA.

that higher harmonic pitch has significant promise for vibration reduction. However, there are potentially complex tradeoffs to be evaluated and managed among the various vibratory hub-load components, as well as blade fatigue loads and rotor performance. The tradeoffs depend directly on the characteristics of the type of rotor--articulated, teetering, or hingeless--and the detailed dynamic characteristics of the particular rotor (especially the placement of the blade modal frequencies relative to the harmonics of shaft speed).

The investigation reported here extends the testing and analysis of the hingeless rotor. This rotor is distinguished by the fact that hub moments (as well as hub forces) are significant contributors to vibration, so that vibration treatment must deal with the vibratory hub moments.

Two previous studies of higher harmonic pitch on hingeless rotors have been performed, both of which involved wind-tunnel testing. The first of these⁶ was limited because model hardware restricted the testing to very low tip speed (61 m/sec or 200 ft/sec) where the blade modal frequencies were not realistic, and because only blade-root loads were measured. Vibratory hub loads, outboard-blade loads, and rotor performance were not available. The second study of hingeless rotors⁹ included testing of a fully instrumented model at higher tip speed (98 m/sec or 320 ft/sec) where the modal frequencies were somewhat more realistic. (ω_{2F}/Ω , for example, was improved from 6.3/rev in Reference 6 to 3.5/rev in Reference 9.) That testing principally involved the reduction of vertical vibratory hub loads, however, and only briefly addressed the reduction of vibratory hub moments. Despite their limitations, both studies were very encouraging and they stimulated the more extensive testing and analysis reported in this paper.

2. Current Wind-Tunnel Testing

Overview

Additional testing of the wind-tunnel model of Reference 9 was conducted in mid-1976 in the 6.1-m by 6.1-m (20- by 20-foot) test section of the Boeing V/STOL wind tunnel. This testing further explored the use of 4/rev swashplate inputs to reduce 4/rev vibratory hub loads of a four-bladed hingeless rotor. The testing was conducted at nearly full-scale tip speed (175 m/sec or 575 ft/sec) with realistic placement of blade modal frequencies. The model was fully instrumented. Three-per-rev, 4/rev, and 5/rev blade pitch were obtained individually with a range of amplitudes and phases, by shaking and whirling the swashplate at 4/rev. Testing was conducted at three advance ratios and two thrust coefficients in trimmed level flight. Using sensitivities determined from this testing, combinations of 3/rev, 4/rev, and 5/rev pitch were then applied in a single trim condition to obtain simultaneous reductions in all components of measured 4/rev hub loads.

Model Rotor

The model rotor, shown in Figure 1 as it was installed in the wind tunnel, is a 3.05-m (10-foot)-diameter, four-bladed, soft-in-plane hingeless rotor. The airfoil is the 12-percent VR-7 to 75 percent of the blade radius, tapered in thickness to the 6-percent VR-9 at the tip. The blades are dynamically scaled to an early version of the full-scale Model 179 hingeless-rotor helicopter developed by the Boeing Vertol Company. The blade modal-frequency map is shown in Figure 2.

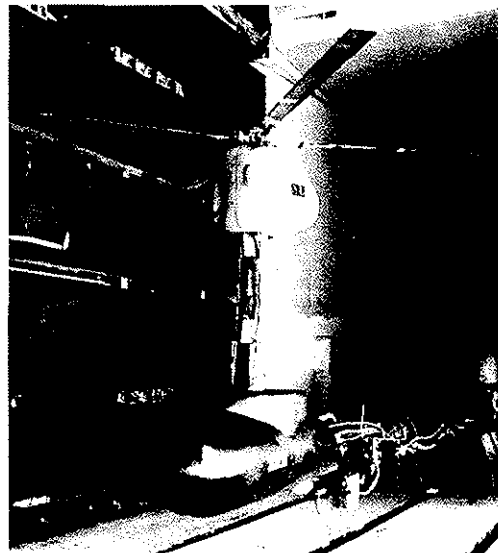


Figure 1. Model Rotor Installed in Wind Tunnel

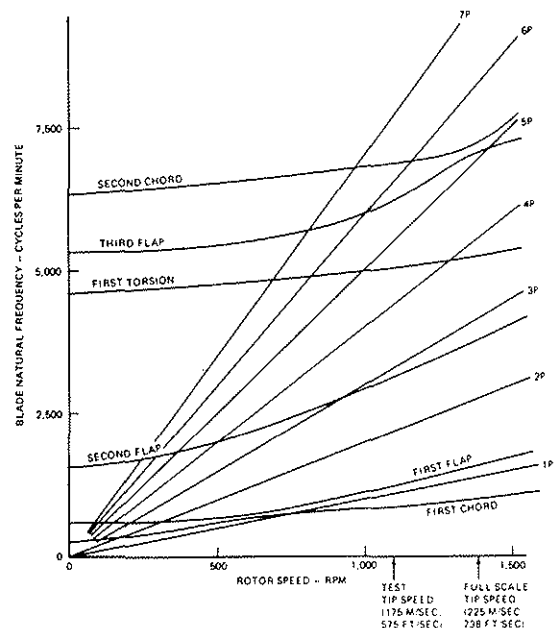


Figure 2. Natural Frequency Spectrum of Model Rotor

Control System

Model shaft speed, shaft angle, and blade pitch were controlled remotely. Blade pitch was controlled by a swashplate positioned by hydraulic actuators. The actuators were driven electrically by commands of conventional collective and cyclic pitch, to which higher harmonic signals could be added. That is, n/rev collective (swashplate vertical shaking), n/rev longitudinal cyclic (swashplate rocking about one nonrotating axis), and n/rev lateral cyclic (swashplate rocking about another nonrotating axis perpendicular to the first) could be superimposed on the normal swashplate positioning. Three n/rev signals of independently controlled amplitude and phase (timing relative to the azimuthal position of a reference blade) were available for input to the collective, longitudinal cyclic, and lateral cyclic control channels. For example, one $4/\text{rev}$ signal could be applied to the collective channel for $4/\text{rev}$ vertical shaking of the swashplate while another $4/\text{rev}$ signal of different amplitude and phase was applied to the longitudinal cyclic channel for $4/\text{rev}$ rocking of the swashplate, and a third $4/\text{rev}$ signal of still different amplitude and phase could be applied to the lateral cyclic channel for $4/\text{rev}$ rocking of the swashplate about the other axis.

Control Inputs for 3/Rev and 5/Rev Pitch

The trigonometric relationship between swashplate angle and blade pitch can be used to show that $4/\text{rev}$ rocking of the swashplate about one axis produces a combination of $3/\text{rev}$ and $5/\text{rev}$ blade pitch variations. If the swashplate is rocked about two perpendicular axes simultaneously, with equal amplitude but 90 degrees phase difference (which amounts to whirling the swashplate at $4/\text{rev}$), the same trigonometry shows that pure $3/\text{rev}$ or pure $5/\text{rev}$ pitch will be produced, depending on the sign of the 90-degree phase difference. That is, if the swashplate is whirled at $4/\text{rev}$ in the same direction as the shaft turns, $3/\text{rev}$ pitch will be produced, whereas whirling in the direction opposite that of the shaft produces $5/\text{rev}$ pitch. Both $3/\text{rev}$ and $5/\text{rev}$ pitch were obtained in this manner during the testing; $4/\text{rev}$ pitch was also obtained by vertical swashplate shaking.

Control Limitations on Model Operation

The sinusoidal output capability of hydraulic actuators decreases rapidly with frequency as a result of valve flow-rate limitations. Such limitations placed serious rpm constraints on earlier testing programs^{6,9}. For this test, simple improvements to the hydraulic system were made to permit testing at much higher rpm. Adequate $4/\text{rev}$ swashplate amplitudes were obtained up to a tip speed of 175 m/sec (575 ft/sec), where blade modal frequencies are much more typical of full-scale designs. For future testing, further model improvements will be made for testing at still higher rpm. (Full-scale application of higher harmonic pitch can similarly be achieved by straightforward control system modifications.)

As shown by Figure 2, testing at a tip speed of 175 m/sec (575 ft/sec) placed the blade modal

frequencies in or close to the normal design range. The test results thus apply to a dynamically realistic rotor configuration.

Instrumentation

The model was fully instrumented to measure steady and high-frequency values of swashplate position, blade-root pitch, blade loads at various spanwise stations, total model loads, and shaft torque. Blade instrumentation included the following gages:

- Flap-bending moment at $r/R = 0.11, 0.16, 0.36, 0.64, 0.68, 0.85$
- Chord-bending moment at $r/R = 0.11$
- Torsional moment at $r/R = 0.18, 0.41, 0.69, 0.87$

Total model loads were measured by a strain-gage balance in the nonrotating system below the control actuators. In this position, the balance was sensitive to swashplate inertial loads. Since the swashplate weight and inertia about a diameter were not scaled like the rotor, proper consideration of the data required subtraction of the excess swashplate inertial loads from the higher harmonic balance loads. This correction was applied to all hub loads derived from balance measurements.

3. Test Conditions and Procedure

In each of the conditions shown in Figure 3, the rotor was trimmed to zero steady hub moment and propulsive-force coefficient $X/qd^2\sigma = 0.10$, representative of steady level flight. As illustrated in Figure 4, the rotor was controlled by setting the collective and cyclic controls for thrust and trim, then adding higher harmonic pitch for vibration reduction. Three-per-rev, $4/\text{rev}$, and $5/\text{rev}$ pitch were applied individually. Each harmonic was applied first at a fixed amplitude while data points were taken for eight different phases from 0 to 360 degrees. For example, a data point was taken for

$$\theta_4 = 0.2 \cos 4\psi \text{ (degrees),}$$

then for $\theta_4 = 0.2 \cos (4\psi - 45^\circ)$,

and for $\theta_4 = 0.2 \cos (4\psi - 90^\circ)$,

and so on. The phase was then set at the value shown by the data to be most favorable for reduction of a selected vibratory hub-load component, and data points were taken for various amplitudes from zero to the maximum available. For example, if interpolation indicated that a favorable phase was 70 degrees, data points were taken for:

$$\theta_4 = 0.05 \cos (4\psi - 70^\circ),$$

$$\theta_4 = 0.10 \cos (4\psi - 70^\circ),$$

$$\theta_4 = 0.15 \cos (4\psi - 70^\circ),$$

.
.
.

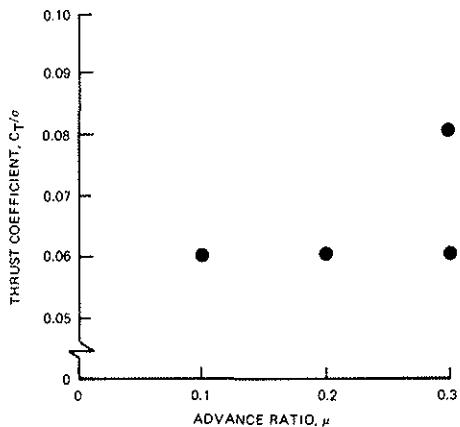


Figure 3. Summary of Test Conditions

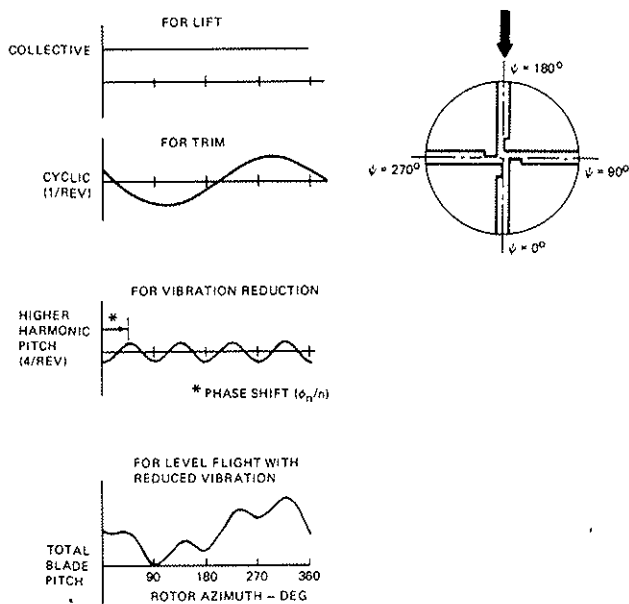


Figure 4. Rotor-Blade Pitch Requirements

As mentioned earlier, one of the trim conditions, $\mu = 0.30$ and $C_T/\sigma = 0.06$, was selected for simultaneous application of 3/rev, 4/rev, and 5/rev pitch to demonstrate superposition of the effects. The goal here was to demonstrate simultaneous reduction of all the vibratory hub-load components.

4. Tests Confirm That Blade Moments and Hub Loads Change Nearly Linearly With Harmonic Control Inputs

Test results confirmed the approximate linearity of higher harmonic pitch effects which was expected on the basis of earlier investigations.

Figure 5, for example, presents the effects of 5/rev pitch on 5/rev blade-root flap-bending moment. (This bending moment is a direct contributor to the 4/rev vibratory hub moments.) The 5/rev bending moments for various pitch amplitudes and phases are plotted in polar format, each data point representing the amplitude and phase of a measured 5/rev bending-moment component. The data points form a distinct pattern: an elliptical grouping (B) surrounding a central point (A), with a somewhat radial line (C) connecting the two. The central point (A) is the 5/rev flap bending measured with no harmonic pitch applied. The outer points (B) represent the 5/rev flap bending measured with a 5/rev pitch input of constant amplitude applied with various phases, which are noted beside the individual points. The points on the line (C) emanating from the central point represent the 5/rev flap bending measured with a 5/rev pitch input of constant phase applied with various amplitudes, which are noted beside the individual points.

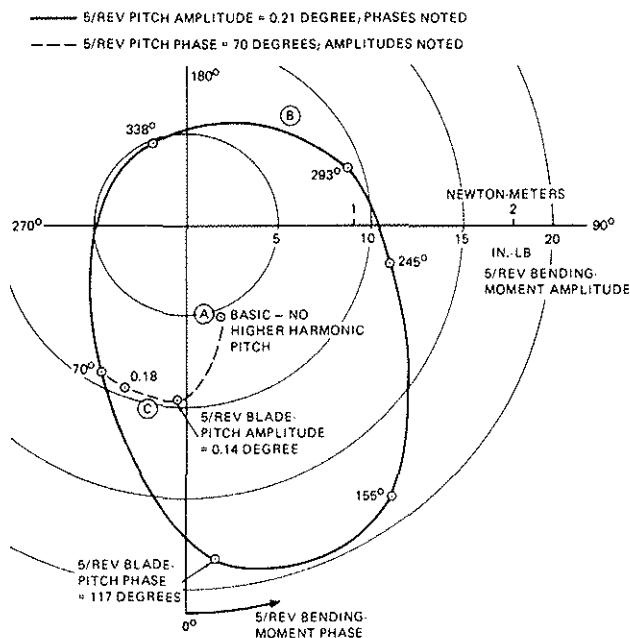


Figure 5. 5/Rev Flap-Bending Moment at $r/R = 0.11$ for 5/Rev Blade-Pitch Inputs of Various Amplitudes and Phases at $\mu = 0.3$ and $C_T/\sigma = 0.06$

It can be observed that all the points in Figure 5, other than the central point (A), are obtained from the central point by adding an incremental flap-bending vector which is almost linearly dependent on the 5/rev pitch input. The points in the elliptical grouping (B), for example, are obtained by adding an incremental vector whose

length is about 0.9 n-m (8 in.-lb) for input phases of 65 or 245 degrees, about 1.4 n-m (12.5 in.-lb) for input phases of 145 or 325 degrees and a weighted average of these two lengths for phases in between. The direction of the incremental vector varies smoothly with the input phase, and a sweep of the input phase from 0 to 360 degrees swings the incremental vector in a complete circle around the baseline point. The points on the line (C) emanating from point (A), on the other hand, are obtained by adding an incremental vector whose direction is relatively constant (like the phase of the 5/rev pitch input), and whose length is approximately proportional to the 5/rev input amplitude. Characteristics such as these are described by a linear equation of the form,

$$\begin{pmatrix} M_{\beta 5c} \\ M_{\beta 5s} \end{pmatrix} = \begin{pmatrix} M_{\beta 5c} \\ M_{\beta 5s} \end{pmatrix}_{\text{BASIC}} + \begin{bmatrix} a_{11} & a_{12} \\ a_{21} & a_{22} \end{bmatrix} \begin{pmatrix} \theta_{5c} \\ \theta_{5s} \end{pmatrix} \quad (1)$$

(Cosine components in equation 1 correspond to vector components in the 0-degree phase direction in Figure 5, while sine components correspond to vector components in the 270-degree phase direction, in keeping with the phase convention established at the beginning of this paper.)

The grouping (B) of Figure 5 is elliptical because, as the phase of the harmonic pitch input changes, the orientation of the harmonic pitch waveform changes relative to the forward-flight velocity and the vortex wake beneath the rotor disk. For some input phase in particular (145 degrees in Figure 5), the harmonic pitch effects add to the local velocity effects to produce the largest incremental loads and the largest incremental moment vector. At the opposite phase (180 degrees different), the interaction is also strong but exactly opposite, producing an almost equally long incremental moment vector in the opposite direction. And for some intermediate input phase and the phase exactly opposite to it (65 and 245 degrees in Figure 5), the interaction is weakest, producing the shortest incremental moment vectors.

In hover, the local wind velocities are constant with azimuth, so the length of the incremental vector is independent of the input pitch phase; thus the grouping (B) is circular. This is confirmed by test data. In this case, the a_{ii} matrix takes the familiar form,

$$\begin{bmatrix} a_{11} & a_{12} \\ a_{21} & a_{22} \end{bmatrix} = \begin{bmatrix} K \cos \gamma & K \sin \gamma \\ -K \sin \gamma & K \cos \gamma \end{bmatrix} \quad (2)$$

In equation 2, K is the ratio of the amplitude of the incremental bending vector to the amplitude of the pitch input, and γ is the differ-

ence between the direction of the incremental vector and the phase of the pitch input.

Given the linear characteristics confirmed by Figure 5, it is clear that the 5/rev pitch amplitude and phase can be adjusted for complete elimination of the 5/rev root flap-bending moment. Interpolation of the Figure 5 data indicates that 0.15 degree amplitude is required at 300 degrees phase. It is also clear that the 5/rev pitch input could be adjusted for approximate elimination of the 5/rev root moment after measuring the effects of two trial 5/rev pitch inputs at different phases. Such measurements would permit the calculation of the a_{ii} elements of equation 1, which could then be inverted to obtain the required 5/rev pitch cosine and sine components.

It can also be noted that the 5/rev pitch input could easily be adjusted to reduce the 5/rev root moment on the basis of a single trial input. This is because the elliptical grouping

(B) of Figure 5 is not extremely eccentric and can

be roughly approximated by a circle. A single trial pitch input would establish a matrix a_{ii} in the form of equation 2 which would correspond to some circular approximation to the grouping (B). In simpler terms, a trial input would establish an approximate ratio (K) between the input harmonic pitch amplitude and the length of the incremental moment vector, and an approximate phase difference (γ) between the input phase and the direction of the incremental moment vector. Thus, when a trial incremental vector was measured, the input phase could be changed by exactly the amount of angular rotation required to point the trial vector at the origin (the zero bending-moment point), and the input amplitude could be multiplied by the scale factor required to make the trial vector exactly reach the origin. These simple adjustments would be totally successful if the grouping (B) were perfectly circular.

Since it is not too far from circular, the simple adjustments would accomplish some reduction in most cases.

The test data showed that the approximate linearity of higher harmonic pitch effects seen in Figure 5 is also characteristic of all the other blade loads. Furthermore, it is characteristic of blade-load components at other harmonics. For example, a diagram like Figure 5 can be drawn for the effects of 5/rev blade pitch on 3/rev root chord bending. Similar diagrams can also be drawn for the effects of the other higher harmonics of pitch, 3/rev and 4/rev.

In view of the approximately linear dependence of all the blade loads on the higher harmonic pitch inputs, the vibratory hub loads must also show an approximate linear dependence. This was confirmed by the test data, an example of which is shown in Figure 6. This diagram, in the same format as Figure 5, shows the effects of higher harmonic blade pitch on 4/rev hub-pitching moment obtained from strain-gage balance measurements.

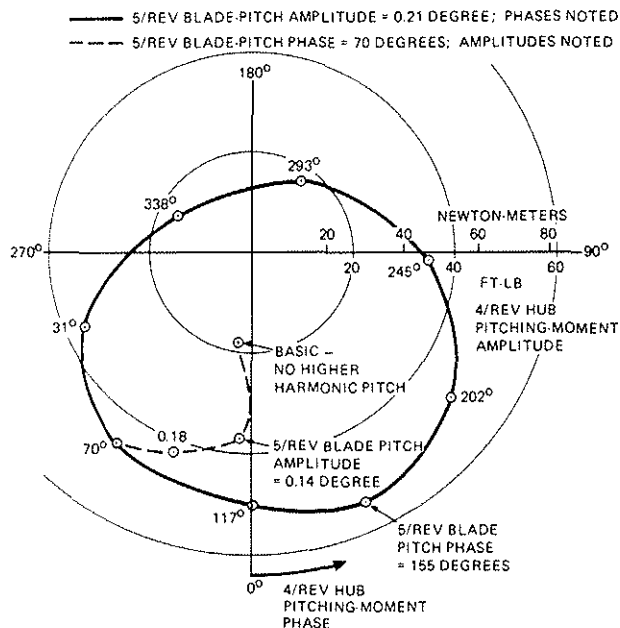


Figure 6. 4/Rev Hub Pitching Moment for 5/Rev Blade-Pitch Inputs of Various Amplitudes and Phases at $\mu = 0.3$ and $C_T/\sigma = 0.06$

5. Tests Show Small Effects on Rotor Performance

The effects of higher harmonic pitch on rotor performance were found to be quite small for all amplitudes and phases tested, amounting to no more than several percent in L/D_e , the lift-to-effective drag ratio. The changes were frequently small improvements. Since some scatter was present in the data, however, quantitative conclusions are suspended until a larger data base becomes available from further testing. In any case, no major performance penalties are expected.

(Substantial performance gains were demonstrated in the Reference 9 testing using 2/rev blade pitch, but such effects were not the object of the current investigation.)

6. Blade Response Data Has Expected Characteristics

The blade-loads data confirms a fundamental expectation about blade response to higher harmonic pitch, namely that the response principally involves the modes whose frequencies are closest to the applied pitch harmonics. Figures 7 and 8, for example, show the effects of 3/rev and 5/rev pitch on the flap-bending and torsional-moment distributions along the blade. Plotted here are the changes in blade loads relative to baseline values; that is, the lengths of the incremental blade-load vectors described in the preceding section. The incremental vectors are found to have generally the same phase, or 180 degrees different phase, all along the span, so that the

amplitudes alone, plotted positive or negative (for 180 degrees out of phase), convey most of the information.

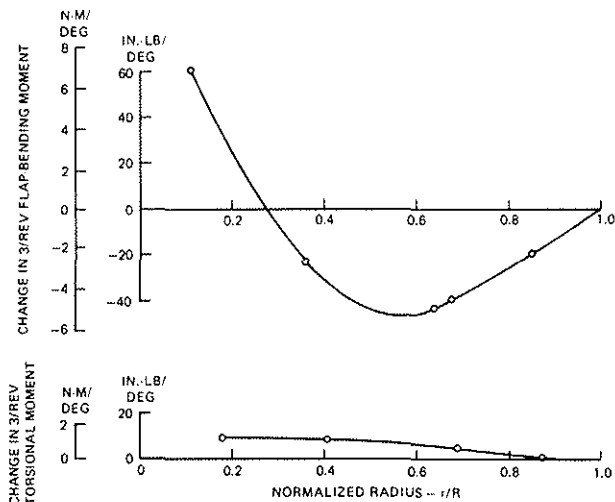


Figure 7. Changes in 3/Rev Blade Loads per Unit 3/Rev Pitch at $\mu = 0.1$ and $C_T/\sigma = 0.06$

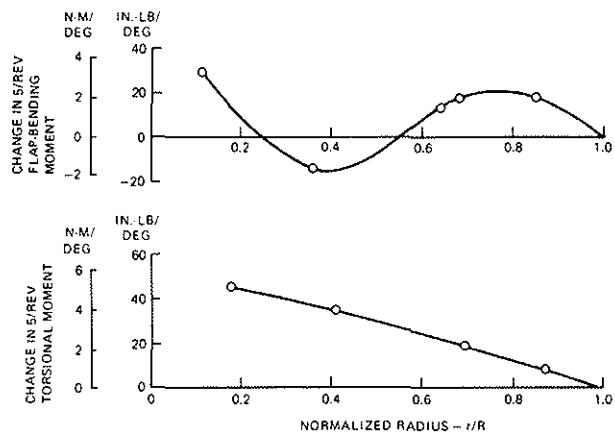


Figure 8. Changes in 5/Rev Blade Loads per Unit 5/Rev Pitch at $\mu = 0.1$ and $C_T/\sigma = 0.06$

Figures 7 and 8 show that the incremental flap-bending response to 3/rev pitch is predominantly in the second flap mode, while the response to 5/rev pitch is predominantly in the third flap mode. The figures also show that the torsional response to 5/rev pitch is much larger than that resulting from 3/rev pitch. This is expected because of the greater proximity of the first torsion mode to 5/rev. The magnitude of the torsional loads indicates that at 5/rev the blade-tip pitching amplitude is approximately four times the amplitude input at the root, whereas at 3/rev the tip and root amplitudes are approximately the same.

7. Theoretical Predictions Agree With Blade Data

Correlation of the incremental flap-bending and torsional-moment response to 5/rev pitch, as measured and as predicted by the Boeing Vertol Rotor Loads Program C-60, is shown in Figure 9. Program C-60 is a coupled flap-torsion, uncoupled lag analysis which employs a lumped-parameter blade model with 20 spanwise blade sections to represent nonuniform distributions of mass and inertia, elastic properties, and geometric characteristics. The aerodynamics are fully nonlinear, and the nonuniform-downwash distribution is calculated by integrating the effects of a spiral vortex wake. Solutions are obtained by an iterative approach which yields a consistent set of downwash, airloads, and blade deflections, taking account of all the significant physical nonlinearities.

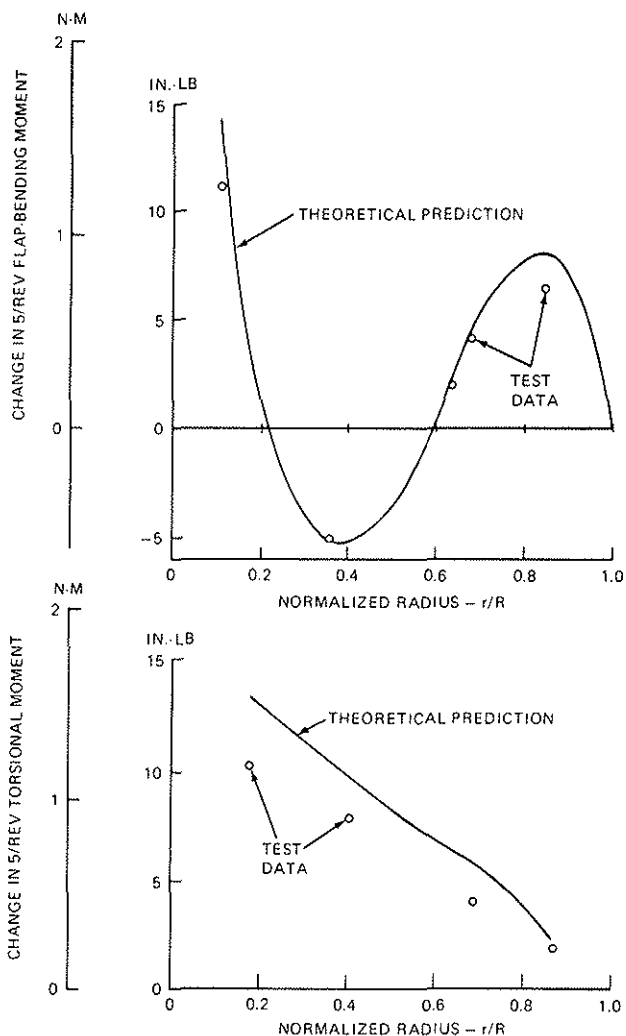


Figure 9. 5/Rev Pitch Effects on Blade Loads--Test Data Versus Theoretical Prediction ($\theta_3 = 0.216^\circ / -22^\circ$ at $\mu = 0.3$ and $C_T/\sigma = 0.06$)

The correlation in flap bending is excellent. Predicted torsional-load changes are conservative by 25 percent since the mathematical model places the torsion mode slightly too close to 5/rev. In general, such correlation increases confidence in the quality of the test data as well as in the theoretical methods.

8. Consistency of Blade and Balance Data

Data consistency was checked in the following way. Four-per-rev hub moments were calculated from the 4/rev balance loads, including a correction for the washplate inertial loads. Then the same 4/rev hub moments were calculated from the 4/rev blade-root flap-bending moments, whose accuracy was supported by the theoretical predictions. Results of the two methods were in close agreement for data points with no higher harmonic pitch, that is, with no washplate shaking. The results differed distinctly, however, when higher harmonic pitch was applied. The difference was such that the incremental 4/rev hub moments calculated from balance measurements were related to those calculated from blade measurements by an approximately constant-amplitude ratio and phase difference for groups of data points taken at the same trim condition. The amplitude ratio and phase difference varied, however, between pitch moments and roll moments and as trim condition was changed, with no apparent pattern.

Hub-moment predictions of Program C-60 generally agree with the calculations made from blade loads. This would be expected because Program C-60 corroborates the measured blade loads themselves. Figure 10 compares results of the two hub-moment calculation methods with the corresponding C-60 prediction for a typical data point.

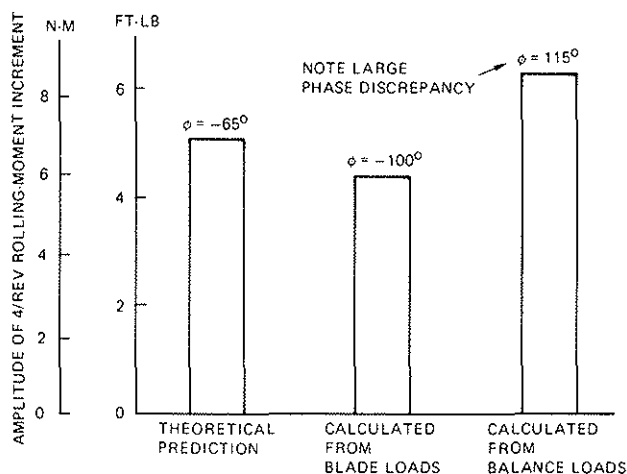


Figure 10. Comparison of 4/Rev Hub Rolling-Moment Changes Calculated by Two Methods With Program C-60 Prediction ($\theta_3 = 0.17^\circ / -125^\circ$ at $\mu = 0.2$ and $C_T/\sigma = 0.06$)

The most likely explanation for the discrepancy in the balance-derived hub loads is that the redundant control actuators were not perfectly synchronized, causing them to oppose each other and apply spurious reactive loads to the balance. Such small desynchronization would certainly have had different results along different axes of the balance, and could have changed slightly as the harmonic signal generator was turned off and on, which would account for different results among different trim conditions.

As a result of this finding, much more careful attention will be given to actuator synchronization and the entire question of balance-load accuracy in future testing. The balance loads measured in this test, because of the consistency within groups of data points, are simply considered illustrative of certain qualitative trends when used appropriately.

9. The Potential Tradeoff Between Blade Loads and Hub Loads

Earlier investigations have revealed that in some applications of the higher harmonic pitch concept, adjustment of the amplitude and phase of the higher harmonic input to achieve hub-load reduction causes significant increases in blade-bending loads. The physical explanation is discussed at length in Reference 3; the problem arises because higher harmonic pitch reduces a harmonic hub load resulting from airloads in one spanwise distribution by cancelling it with an opposing hub load produced by incremental airloads in a different spanwise distribution; that is, cancellation of loads at the root of the blade can be accompanied by increase of loads on the rest of the blade because the incremental loads used for the cancellation are not necessarily distributed along the span in the same way as the basic loads. The loads involved are not only aerodynamic; there are basic and incremental inertial loads as well, associated with blade harmonic motion. It is the distribution of total loads--aerodynamic plus inertial--which establishes the relationship between the hub-load and blade-load effects of higher harmonic pitch.

McCloud and Kretz^{5,7} have described an excellent systematic approach to dealing with hub-load/blade-load tradeoffs which minimizes a weighted average of various hub- and blade-load parameters. McCloud⁷ explored the tradeoffs and demonstrated the approach analytically for an articulated rotor. The hingeless rotor has not been investigated from this viewpoint, however, except for the limited consideration in Reference 9.

The desire to avoid tradeoffs entirely has led to some consideration of partial spanwise harmonic pitch, in contrast to higher harmonic pitch applied to the entire blade. Various amounts of spanwise shaping of the incremental harmonic loads can be conceived, each with its own price in both hardware and control complexity. The most desirable spanwise shaping would vary with trim and maneuver condition, since the spanwise distribution of the basic vibratory loads varies with these conditions.

Fixed or variable spanwise shaping of the higher harmonic pitch input could be mechanically simpler if it were achieved by flap or tab devices, or by aerodynamic methods of lift control involving blowing, rather than by pitching of independent blade elements. All approaches are somewhat complex at best, however, so it is of great interest to explore the hub-load/blade-load tradeoffs for a particular rotor, with the hope that simple methods of harmonic pitch application will be successful.

10. Pertinent Characteristics of Hingeless Rotors

There is one blade dynamic feature which tends to reduce the need for spanwise shaping of the higher harmonic pitch input. This is heavy involvement of a single blade-bending mode in the response to the higher harmonic input, as well as in the response to the basic airloads at that harmonic. Such involvement first tends to make the inertial loads predominate over the aerodynamic loads, both basic and incremental. Then, since the same mode is involved in the basic blade motion and the incremental blade motion, the basic and incremental load distributions tend to be similar.

A four-bladed hingeless rotor has advantages in this respect. Four-per-rev hub moments are important targets for vibratory load reduction, and these arise from 3/rev and 5/rev blade flapwise bending; the second flap-bending mode is usually heavily involved in 3/rev blade flap bending, while the third flap-bending mode is heavily involved in 5/rev blade flap bending, as shown in Section 6. This gives encouragement that the hingeless rotor will not experience serious increases of outboard flap-bending moments as a side effect of 4/rev hub-moment reduction by higher harmonic pitch applied at the blade root. In fact, this favorable expectation was confirmed for the model rotor at every trim condition shown in Figure 3, as described in the following section.

11. Test Data Indicates Hub Moments Can Be Reduced Without Blade-Load Penalty

Typical examples of blade bending-moment distributions on the model rotor are shown in Figures 11 and 12, which apply to transition flight at $\mu = 0.1$ and $C_{Tq}/\sigma = 0.06$. The figures compare the distributions of the basic flap-bending moments and the incremental flap-bending moments for harmonic inputs of favorable phase at both 3/rev and 5/rev. For the bottom third of each figure, the incremental distributions were scaled (i.e., the test data was linearly interpolated or extrapolated) in the amount necessary to achieve perfect cancellation of the harmonic loads at the blade root and added to the basic distributions. This yielded the residual spanwise moment distributions that would accompany complete elimination of 4/rev hub moments. Figure 11 shows that the 3/rev distributions are fairly well matched; perfect cancellation of the 3/rev root flap-bending moment is accompanied by a small increase, about 7 percent, in the maximum outboard 3/rev flap-bending moment.

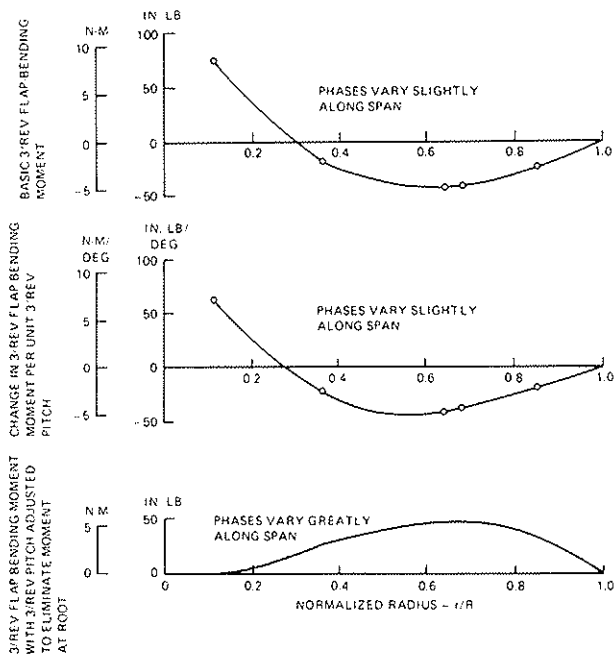


Figure 11. Effect of 3/Rev Root-Moment Elimination on 3/Rev Flap-Bending Moments Along the Span at $\mu = 0.1$ and $C_T/\sigma = 0.06$

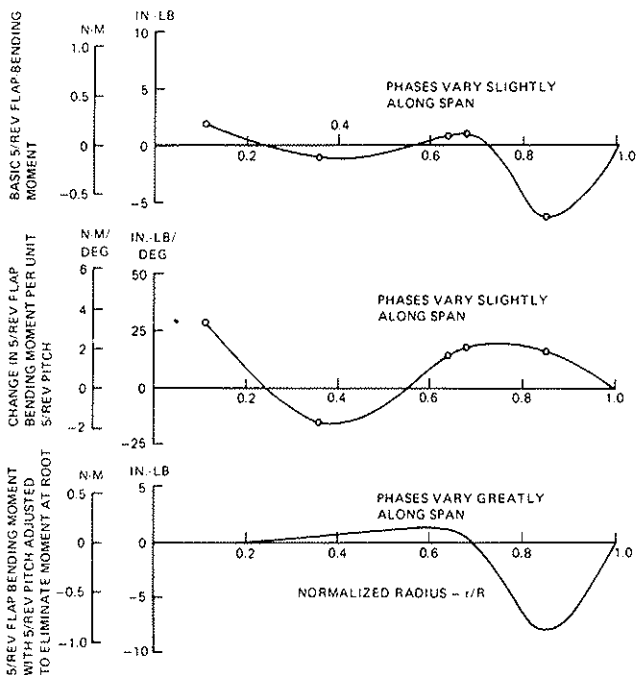


Figure 12. Effect of 5/Rev Root-Moment Elimination on 5/Rev Flap-Bending Moments Along the Span at $\mu = 0.1$ and $C_T/\sigma = 0.06$

Figure 12 shows that the 5/rev distributions are not matched as well because the basic moment distribution contains a peak near the blade tip in addition to the third mode-bending shape. Such peaks are characteristic results of the highly irregular transition downwash distribution. As a result of this irregularity, Figure 12 shows that perfect cancellation of the 5/rev root flap-bending moment is accompanied by a 19-percent increase in the 5/rev peak near the tip. Neither the 3/rev nor the 5/rev bending moments are a predominant part of the total vibratory moments, however, so the effect on the total is small. Figure 13 shows, in fact, that simultaneous cancellation of both the 3/rev and 5/rev root flap-bending loads (i.e., total elimination of 4/rev hub moments) increases the maximum outboard vibratory flap-bending moment by only 2 percent. Comparable results were obtained in every trim condition tested.

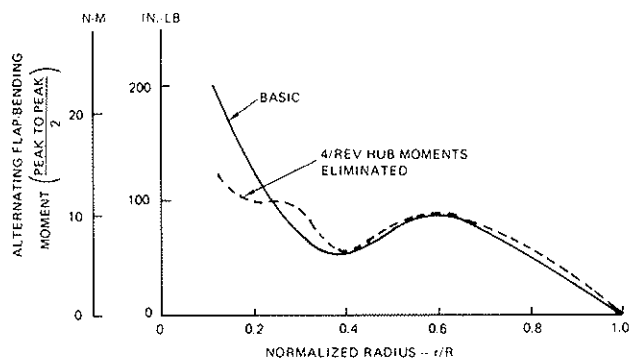


Figure 13. Effect of 4/Rev Hub-Moment Elimination on Total Flap-Bending Fatigue Loads at $\mu = 0.1$ and $C_T/\sigma = 0.06$

12. Calculated Inputs for Vibratory Hub-Moment Reduction Versus Flight Speed

An important concern in the application of higher harmonic pitch for vibration reduction is the extent to which the required inputs vary with flight condition. This characteristic will determine the complexity of the control system needed for in-flight adjustment of the pitch amplitude and phase. The test data permits an initial evaluation for the case of hub-moment reduction on the four-bladed hingeless rotor.

As noted in Section 11, distributions like those of Figures 11 and 12 were prepared for every trim condition tested. The 3/rev and 5/rev pitch amplitude and phase required for perfect cancellation of the blade-root moment at the same harmonic could be calculated from the amount by which it was necessary to scale and adjust the phase of the root-moment increment obtained from the trial input. Such linear interpolation and extrapolation of the data has its limitations, of course, but the results are accurate on the basis of the relatively linear characteristics shown in Figure 5.

Figures 14 and 15 show the amplitude and phase of 3/rev and 5/rev pitch required to completely eliminate the 3/rev and 5/rev blade-root flap-bending moments (and thus the 4/rev vibratory hub moments) at three advance ratios. It should be noted that these requirements were determined independently for each harmonic; they are therefore somewhat inaccurate because they ignore the small effect that 5/rev pitch has on 3/rev loads, changing the 3/rev pitch requirement, and vice versa. The 3/rev pitch, being considerably larger, will have greater effects on 5/rev loads than the 5/rev input will have on the 3/rev loads. For this reason the 3/rev requirement is probably quite dependable, the 5/rev much less so. Nevertheless, the results are instructive and indicative of certain basic features of the in-flight adjustment requirement.

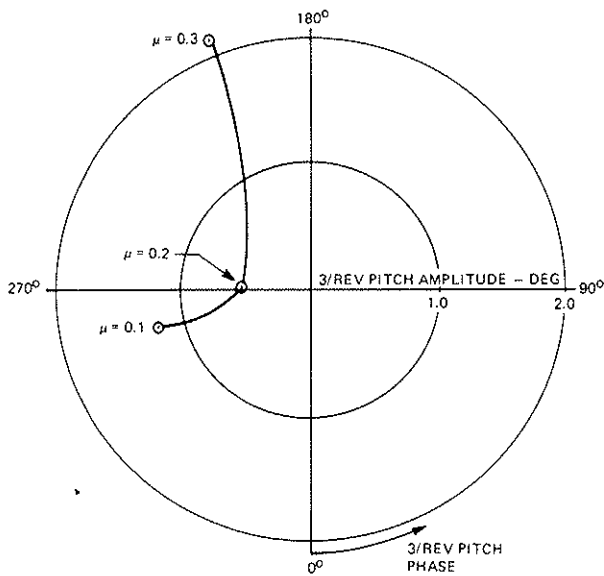


Figure 14. Effect of Advance Ratio in Trimmed Level Flight on 3/Rev Pitch Required to Eliminate 3/Rev Root Flap-Bending Moment

Figures 14 and 15 show first that the 3/rev pitch requirement is an order of magnitude larger than the 5/rev pitch requirement. This is fundamentally due to the much larger size of the 3/rev baseline loads. It suggests, in fact, that the 5/rev requirement could be ignored in many cases to achieve a simpler system with results nearly as favorable.

The figures also show that the amplitudes of the 3/rev and 5/rev pitch requirements decrease from transition ($\mu = 0.1$) to moderate speed ($\mu = 0.15$ or 0.20), then rise again as speed increases. At the same time, there is a 90-degree shift in both the 3/rev and 5/rev phase requirements between transition and high speed. The data shows that the amplitude and phase trends shown in the

figure are predominantly due to trends in the basic 3/rev and 5/rev loads; the incremental loads per unit of higher harmonic pitch input do vary with speed, but less so than the basic loads.

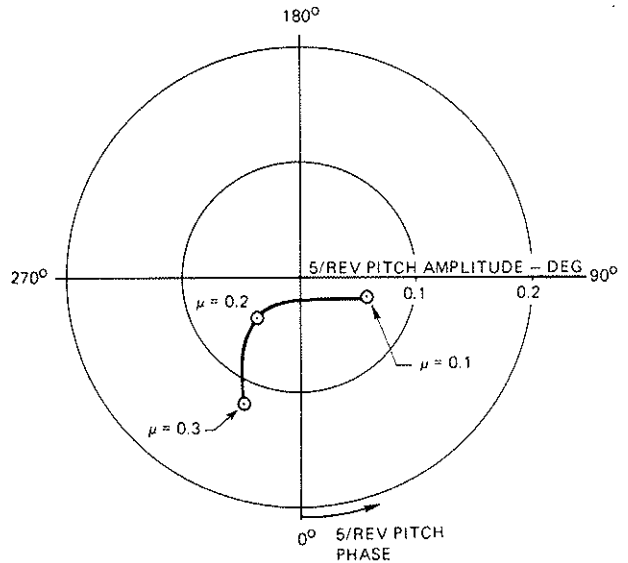


Figure 15. Effect of Advance Ratio in Trimmed Level Flight on 5/Rev Pitch Required to Eliminate 5/Rev Root Flap-Bending Moment

The substantial variation of the required inputs with flight speed permits an initial conclusion about in-flight adjustment. Adjustment of both amplitude and phase will be necessary. An adjustment system which, for simplification, left either of these parameters constant at some compromise value in all conditions could fail to improve vibration, or even make it worse, in certain important flight regimes. Fixing 3/rev phase at the ideal for high-speed improvement, for example, would cause an inaccuracy of approximately 90 degrees in transition; this would degrade transition vibration. More investigation of the higher harmonic requirements as they vary with trim and maneuver is clearly required, however, for design of an adequate and efficient in-flight adjustment mechanism. Open-loop and closed-loop systems are both viewed as possibilities, each having its own advantages and problems.

13. Combined Harmonic Inputs Reduce All Hub-Load Components

In testing higher harmonic pitch, it is significant to demonstrate that several harmonic inputs can be combined for simultaneous reduction of all the vibratory hub-load components. For the hingeless rotor, it is also significant to explore the relationship between hub-moment reduction and in-plane load reduction. This is because the same pitch harmonics would naturally be used to control both the hub moments and the in-plane loads. On a four-bladed hingeless rotor, for example, the 4/rev hub pitching and rolling moments arise dir-

ectly from the 3/rev and 5/rev blade-root flap-bending moments, which are most directly controlled by 3/rev and 5/rev blade pitch; at the same time, however, the 4/rev longitudinal and lateral in-plane hub loads arise directly from the 3/rev and 5/rev blade-root chordwise shears, which are also most directly controlled by 3/rev and 5/rev blade pitch. Thus, there is a question of compatibility between the 3/rev and 5/rev pitch-amplitude and phase adjustments desirable for hub-moment reduction and the adjustments desirable for in-plane load reduction.

Combination of multiple harmonic inputs and compatibility of adjustment strategies were explored during this test using vibratory hub loads calculated from balance measurements. Until the accuracy of the balance measurements is improved, as described in Section 8, this balance data is the most accurate information available about the effects of higher harmonic pitch on the in-plane loads. (The calculation of in-plane hub loads from blade-load data is considerably more complex than the calculation of hub moments and has not been completely developed.) Rather than using in-plane hub loads derived from the balance together with other hub-load components derived from blade loads, it was desirable to use an entirely compatible set of hub loads all derived from the balance. In view of the issues raised in Section 8, however, it will be necessary to confirm the resulting conclusions by additional testing.

For $C_T/\sigma = 0.06$ at $\mu = 0.3$, a set of 3/rev, 4/rev, and 5/rev pitch inputs favorable for 4/rev hub-load reduction was chosen from the set of trial inputs of each individual harmonic. The three pitch harmonics were applied simultaneously. Small amplitude and phase adjustments were made to achieve minor improvements in loads. The results for the full set of 4/rev vibratory hub loads are shown in Figure 16.

The simultaneous reduction of all hub-load components shown in Figure 16 demonstrates that several higher harmonic pitch effects can be superimposed. The simultaneous reduction of the hub moments and in-plane loads in particular demonstrates the compatibility of 3/rev and 5/rev pitch requirements for these purposes.

14. Conclusions

This test has provided further encouragement that higher harmonic blade pitch can be successfully applied for vibration reduction for the specific case of the hingeless rotor. The data shows that:

1. Reduction of vibratory hub loads involves no significant blade flap-bending or rotor-performance penalties over the range of trim conditions tested.

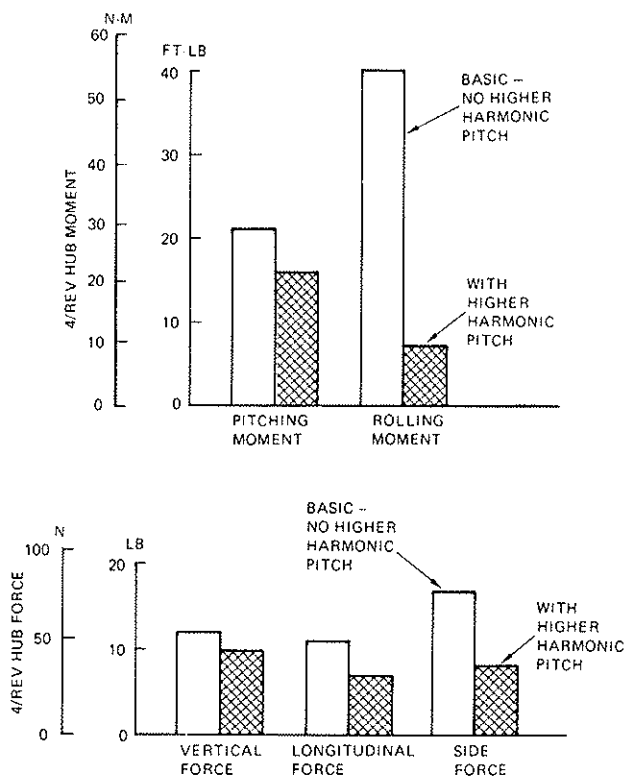


Figure 16. Simultaneous Reduction of All 4/Rev Hub-Load Components Achieved With Combination of 3/Rev, 4/Rev, and 5/Rev Pitch

2. The higher harmonic inputs required to eliminate the 4/rev hub moments of a four-bladed hingeless rotor are on the order of 1.0 degree at 3/rev and 0.1 degree at 5/rev.
3. Simultaneous reduction of several vibratory hub-load components is possible, because the effects of several harmonic pitch inputs can be superimposed.
4. Simultaneous reduction of all vibratory hub-load components appears to be possible because the 3/rev and 5/rev pitch-amplitude and phase requirements for hub-moment reduction and in-plane force reduction are compatible.
5. In-flight adjustment of both amplitude and phase of higher harmonic pitch will be necessary.
6. The amplitude and phase of higher harmonic pitch can be adjusted for approximate elimination of any vibratory hub-load component simply by considering the effects of two trial inputs of different phases, because the effects are approximately linear.

7. The amplitude and phase of higher harmonic pitch can be adjusted for substantial reduction of any vibratory hub-load component on the basis of a single trial input.

Analysis of the data has shown further that:

8. The effects of higher harmonic pitch on blade bending and torsional loads can be predicted quite well with state-of-the-art theory.
9. Exceptional care is required for accurate measurement of hub vibratory loads by a strain-gage balance in the presence of swashplate shaking on a wind-tunnel model.

References

1. AN EXPERIMENTAL INVESTIGATION OF A SECOND HARMONIC FEATHERING DEVICE ON THE UH-1A HELICOPTER, Bell Helicopter Company, Fort Worth, Texas; TR62-109, U.S. Army Air Mobility Research and Development Laboratory, Fort Eustis, Virginia, June 1963.
2. Daughaday, Hamilton, SUPPRESSION OF TRANSMITTED HARMONIC ROTOR LOADS BY BLADE PITCH CONTROL, Cornell Aeronautical Laboratories; TR67-14, U.S. Army Air Mobility Research and Development Laboratory, Fort Eustis, Virginia, November 1967, AD665430.
3. Shaw, John, HIGHER HARMONIC BLADE PITCH CONTROL FOR HELICOPTER VIBRATION REDUCTION: A FEASIBILITY STUDY, Aeroelastic and Structures Research Laboratory Report ASRL 150-1, Massachusetts Institute of Technology, Cambridge, Massachusetts, December 1968, AD702773.
4. Balcerak, John C., and Erickson, John C., Jr., SUPPRESSION OF TRANSMITTED HARMONIC VERTICAL AND INPLANE ROTOR LOADS BY BLADE PITCH CONTROL, Cornell Aeronautical Laboratories; TR69-39, U.S. Army Air Mobility Research and Development Laboratory, Fort Eustis, Virginia, July 1969, AD860352.
5. McCloud, John L., III, and Kretz, Marcel, MULTICYCLIC JET-FLAP CONTROL FOR ALLEVIATION OF HELICOPTER BLADE STRESSES AND FUSELAGE VIBRATION, Proceedings of the AHS/NASA-Ames Specialists' Meeting on Rotorcraft Dynamics, February 1974 (NASA SP352, February 1974).
6. Sissingh, G. J., and Donham, Robert E., HINGELESS ROTOR THEORY AND EXPERIMENT ON VIBRATION REDUCTION BY PERIODIC VARIATION OF CONVENTIONAL CONTROLS, Proceedings of the AHS/NASA-Ames Specialists' Meeting on Rotorcraft Dynamics, February 1974 (NASA SP352, February 1974).
7. McCloud, John L., III, AN ANALYTICAL STUDY OF A MULTICYCLIC CONTROLLABLE TWIST ROTOR, Proceedings of the 31st Annual National Forum of the American Helicopter Society, Washington, DC, May 1975.
8. Kretz, Marcel, RESEARCH IN MULTICYCLIC AND ACTIVE CONTROL OF ROTARY WINGS, Proceedings of the 1st European Rotorcraft Forum, Southampton, England, September 1975.
9. McHugh, Frank J., and Shaw, John, BENEFITS OF HIGHER HARMONIC BLADE PITCH: VIBRATION REDUCTION, BLADE LOAD REDUCTION, AND PERFORMANCE IMPROVEMENT, Proceedings of the American Helicopter Society Midwest Region Symposium on Rotor Technology, August 1976.